Amino Acids (2007) 33: 305–313
DOI 10.1007/s00726-007-0527-y
Printed in The Netherlands

Amino Acids

Structure-activity investigations of polyamine-anthracene conjugates and their uptake via the polyamine transporter

O. Phanstiel IV[1], **N. Kaur**[1], and **J.-G. Delcros**[2]

[1] Department of Chemistry, University of Central Florida, Orlando, FL, USA
[2] CNRS UMR6061 ''Génétique & Dévelopement'', Cell Cycle Group, Faculté de Médecine, Université Rennes, Rennes, France

Received October 20, 2006
Accepted February 1, 2007
Published online April 6, 2007;

Summary. A series of polyamine conjugates were synthesized and evaluated for their ability to target the polyamine transporter (PAT) in two Chinese hamster ovary (CHO) cell lines (PAT-active CHO and PAT-inactive CHOMG). This systematic study identified salient features of the polyamine architecture required to target and enter cells via the PAT. Indeed, the separation of charges, the degree of *N*-alkylation, and the spacer unit connecting the N^1-terminus to the appended cytotoxic component (anthracene) were found to be key contributors to optimal delivery via the PAT. Using the CHO screen, the homospermidine motif (e.g., 4,4-triamine) was identified as a polyamine vector, which could enable the selective import of large N^1-substituents (i.e., naphthylmethyl, anthracenylmethyl and pyrenylmethyl), which were cytotoxic to cells. The cell selectivity of this approach was demonstrated in B-16 murine melanoma cells and normal melanocytes (Mel-A). Three polyamine areas (recognition and transport, vesicle sequestration and polyamine-target interactions) were identified for future research.

Keywords: Polyamine – Transport – Anthracene – Cytotoxicity

Abbreviations: AZ, Antizyme; CHO, chinese hamster ovary; CHOMG, polyamine transport deficient CHO cells; DFMO, α-difluoromethylornithine; Mel-A, normal melanocyte cell line; MGBG, methylglyoxal-bis(guanylhydrazone); ODC, ornithine decarboxylase; PAT, polyamine transporter; SPD, spermidine

Introduction

Polyamines (putrescine, spermidine and spermine, see Fig. 1: **1**, **2a**, **3a**) are ubiquitous low-molecular-weight alkylamines bearing multiple amine groups. These compounds are required in many cellular processes. At physiological pH, they exist as polycations, and likely function via their interactions with anionic biomolecules (e.g., DNA, RNA, phospholipds and proteins). Their intracellular levels are tightly controlled by a machinery that allows rapid and efficient fluctuations in order to respond to specific needs as well as to avoid excessive accumulation of these intrinsically toxic compounds.

In contrast to inorganic cations, polyamines can be biosynthesized and metabolized. Intracellular levels of polyamines are maintained by a subtle equilibrium between a complex enzymatic machinery (controlling biosynthesis, degradation and retroconversion of these amines), and systems that allow import and export of polyamines. Although the molecular biology of polyamine metabolism in mammalian cells is extensively known, polyamine transport remains an observable, yet poorly understood, phenomena. The identity of the mammalian polyamine transporter(s) (PAT) is still unknown and, in fact, the nature of the system itself is a 'black box'.

Most mammalian cells take up polyamines by carrier-mediated, sodium- and energy-dependent mechanisms. Many cells appear to have a single transporter for the three polyamines while, in certain cells, separate transporters have been identified. The PAT is also fully integrated into the cellular regulatory system for the control of intracellular polyamine levels. Detailed reviews of this regulatory system have been published (Seiler and Dezeure, 1990; Seiler et al., 1996).

A key regulator of the PAT activity is antizyme (AZ), a protein that controls the activity of ornithine decarboxylase (ODC). Antizyme is synthesized in response to elevated cellular polyamine levels, binds ODC and promotes its degradation by the proteasome. AZ also plays a role in the feedback control of the PAT activity by a still unknown mechanism (Mitchell et al., 2004).

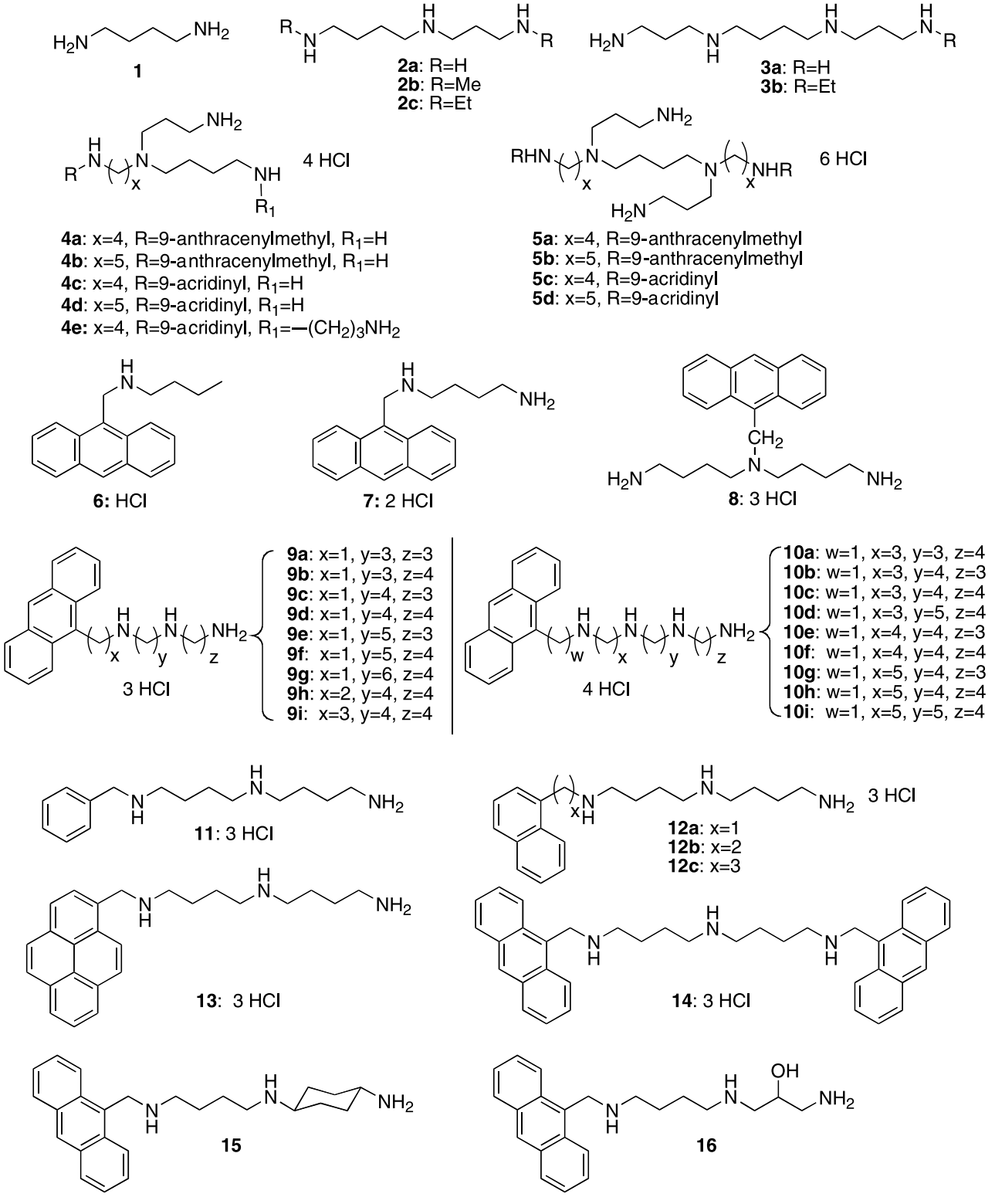

Fig. 1. Native polyamines **1**–**3** and structures of polyamine conjugates, **4**–**16**

Nevertheless, polyamines are able to be transported across the lipophilic cell membrane. How do highly-charged materials accomplish this feat? The model supported by Fransson and his collaborators (Belting et al., 1999, 2003) (Model A in Scheme 1) describes as a first step of the process, the interaction of the charged polyamine with a

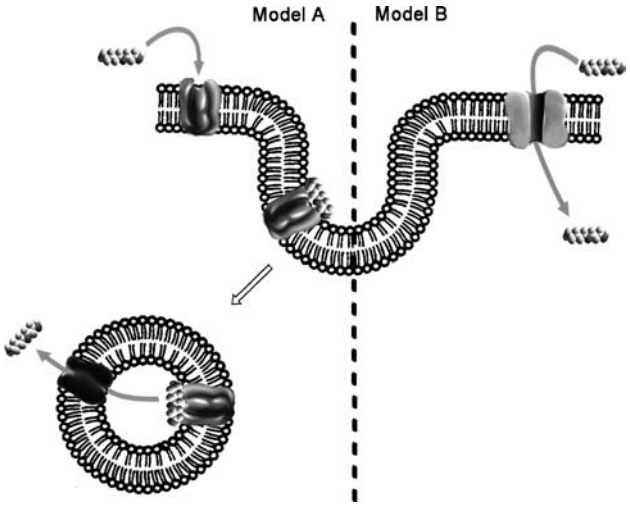

Scheme 1. Two models for the import of polyamines into mammalian cells

negatively charged structure present on the external side of the cell membrane. Heparan sulfate on the proteoglycan glypican-1 has been proposed as the polyamine binding site. The membrane-bound polyamine is then taken into cells through endocytosis. Initial work performed by Poulin and his collaborators (Soulet et al., 2002) using polyamines conjugated to fluorescent probes, which were designed to explore polyamine transport and polyamine intracellular trafficking, also suggested receptor-mediated endocytosis as a route for polyamine entry. However, the same authors recently provided more evidence in favor of a classical transporter (Model B in Scheme 1) requiring an electronegative membrane potential (Soulet et al., 2004). However, it must be kept in mind that these conclusions were drawn from studies made with conjugated polyamines, and up to now, it has never been clearly demonstrated that these polyamine conjugates behave similarly to their free counterparts.

Nevertheless, knowledge of how polycationic materials are imported and sequestered inside mammalian cells could lead to new drug-delivery and gene-delivery technologies, which are cell-selective (Blagbrough and Geall, 1998; Azzam et al., 2002; Gardner et al., 2004, 2007). Moreover, insights gained from polycation-transport studies can be applied to the design of a polyamine pharmacophore, which targets cells via their polyamine-transport activity (Bergeron et al, 2003; Wang et al., 2003a–c; Gardner et al., 2004).

The selection process itself is predicated upon the polyamine import activity of the cell. Many tumor types have been shown to contain not only elevated polyamine levels, but also an activated polyamine transporter (PAT) for importing exogenous polyamines (Seiler et al., 1990, 1996; Cullis et al., 1999). These range from neuroblastoma, melanoma, human lymphocytic leukemia, colonic and lung tumor cell lines to murine L1210 cells (Porter et al., 1984, 1985; Bergeron et al., 1994, 1995, 1997; Cullis et al., 1999; Phanstiel et al., 2000; Wang et al., 2003a–c). Due to the enhanced cellular need for these amine growth factors and an activated transport system for their import, one can deliver polyamine-drug conjugates to specific cell types (Cohen et al., 1992; Bergeron et al., 1994, 1997; Aziz et al., 1998; Casero et al., 2001; Wang et al., 2003a–c; Gardner et al., 2004). This is possible due to particular structural tolerances of the PAT, which allows for import of non-native polyamine constructs (Covassin et al., 1999; Bergeron et al., 2000; Soulet et al., 2002; Delcros et al., 2002; Martin et al., 2001, 2002; Wang et al., 2003a–c; Gardner et al., 2004). Therefore, the PAT is an alternative mode of entry into cells, which can be harnessed for the selective delivery of chemotherapeutics. The 'vectorization' or targeting of chemotherapeutic drugs via attached polyamines is expected to enhance the drug conjugate's cytotoxicity to tumor cells via preferential uptake and to diminish secondary effects on normal cells (Cullis et al., 1999; Gardner et al., 2004).

These characteristics have led to the design of polyamines conjugated to known anticancer agents such as chloroambucil (Holley et al., 1992a; Stark et al., 1992; Cullis et al., 1995), nitroimidazole (Holley et al., 1992b) and aziridine (Heston et al., 1985; Yuan et al., 1994). Some polyamine-drug conjugates showed improved therapeutic indexes. However, the ability of these conjugates to use the PAT to accumulate tumor cells was poorly documented.

In most studies, conclusions were based only upon indirect arguments such as (i) the ability of the conjugates to inhibit the transport of radiolabeled polyamines, (ii) the synergistic effect of α-difluoromethylornithine (DFMO), an inhibitor of ornithine decarboxylase which boosts the PAT activity, or (iii) their reduced cytotoxicity in presence of exogenous polyamines. However, none of these arguments are completely satisfactory. Indeed, polyamine analogs and conjugates with high affinity for the PAT, which are virtually impermeant or are substrates for a cell transport system distinct from the PAT have been reported (Byers and Pegg, 1990; Huber et al., 1996; Delcros et al., 2002, 2006). Historically, the nM K_i values associated with tetraamines implied that they were better substrates for the PAT. However, recent studies have shown that tetraamines irreversibly stick to membrane surfaces, which can introduce bias to the K_i measurement (Wang et al., 2003b). In addition, DFMO is known to have a synergistic effect on

therapeutic drugs, which are structurally unrelated to polyamines (Marton et al., 1981).

To date, significant work has lead to the characterization of the PAT in bacteria, yeast (Igarashi and Kashiwagi, 1999) and, more recently, protozoan parasites (Hasne and Ullman, 2005). In mammals, no proteins have yet been identified. The lack of molecular information has hampered the rational design of PAT-selective polyamine-drug conjugates, and misconceptions have slowed progress.

Our challenge was to design a collection of model compounds that could help identify the molecular recognition elements involved in polyamine transport and to delineate the structural tolerance accommodated by the PAT. These structural elements could be used in a second step, to design more selective, anticancer agents.

Our strategy began with the synthesis of a variety of anthracene-polyamine conjugates. These molecules were fluorescent, cytotoxic and readily accessible via organic synthesis. A series of polyamine-anthracene conjugates were generated in order to deconvolute what polyamine "message" was best recognized by the PAT and what N^1-substituents ("cargoes") could be successfully delivered via the PAT. Insights gained from these experiments have led to a descriptive model of PAT-selective ligands (Gardner et al., 2004).

Materials and methods

Synthesis

The synthesis and characterization of these polyamine conjugates have been described in detail (Phanstiel et al., 2000; Wang et al., 2001, 2003a–c; Gardner et al., 2004). Typically, reductive amination of 9-anthraldehyde with the appropriately-protected amine gave ready access to the desired framework (Wang et al., 2003a). An alternative approach relied on constructing the polyamine sequence stepwise, via an aminoalcohol strategy (Kuksa et al., 2000). The compounds are shown in Fig. 1. Once in hand, the molecular library was screened in Chinese hamster ovary (CHO) cells and its PAT-deficient mutant, CHO-MG (Mandel and Flintoff, 1978).

Bioevaluation

The cell growth and IC_{50} determination protocols in CHO, CHO-MG, B16 and Mel-A cells have been described in detail (Wang et al., 2003a–c; Gardner et al., 2004). Briefly, CHO and CHO-MG, cells were grown in RPMI medium supplemented with 10% fetal calf serum, glutamine (2 mM), penicillin (100 U/ml), streptomycin (50 μg/ml). L-Proline (2 μg/ml) was added to the culture medium for CHO-MG cells. Cells were grown at 37 °C under a humidified 5% CO_2 atmosphere, except B16 and Mel-A cells which were grown under 10% CO_2. Aminoguanidine (2 mM) was added to the culture medium to prevent oxidation of the drugs by the enzyme (bovine serum amine oxidase) present in calf serum. Trypan blue staining was used to determine cell viability before the initiation of a cytotoxicity experiment. Cells in early to mid log-phase were used.

IC_{50} determinations

Cell growth was assayed in sterile 96-well microtiter plates (Becton-Dickinson, Oxnard, CA, USA). CHO and CHO-MG cells were plated at $2e^3$ cells/ml. B16 cells and Mel-A cells were plated at $7e^2$ and $5e^3$ cells/ml, respectively. Drug solutions (10 μl per well) of appropriate concentration were added after an overnight incubation for the cells. After exposure to the drug for 48 h, cell growth was determined by measuring formazan formation from 3-(4,5-dimethylthiazol-2-yl)2,5-diphenyltetrazolium using a Titertek Multiskan MCC/340 microplate reader for absorbance (540 nm) measurements. For B16 and Mel-A, cell growth was determined after 24, 48 and 72 h exposure to the respective conjugates (Gardner et al., 2004).

Fluorescence studies

Culture flasks were seeded at $2e^5$ cells/ml (CHO or CHOMG) in complete medium containing aminoguanidine (2 mM). The respective conjugates (as sterile stock solutions in 0.9% NaCl) were added to the flasks 24 h after the initial seeding at sequential doses ranging from 0.01 to 100 μM, respectively. For the spermidine protection experiment with **9d** in Fig. 2, spermidine (final conc. 200 μM) was added at the same time as the drug addition.

After incubating 24 h, the cells were harvested and washed in cold 0.9% NaCl then sonicated in 0.8 ml of a 0.2 N $HClO_4$/1 N NaCl solution to facilitate the extraction process and the proteins precipitated. The mixture was stored overnight at 4 °C. The samples were centrifuged (10 min at 3000 rpm) and the supernatant saved for fluorescence analysis, while the remaining pellets were saved to determine protein content using the Lowry method after dissolution in 0.1 N NaOH (Lowry et al., 1951).

The quantity of conjugate was determined by fluorescence measurements using calibration curves predetermined with pure material in the 0.2 N perchloric acid/1 N NaCl solution. The excitation and emission maximal wavelengths were slightly different between **9d**, **9h**, and **9i** in 0.2 N $HClO_4$/1 N NaCl. The excitation maximal wavelength for **9d**, **9h** and **9i** were 365, 368 and 369 nm, respectively. Emission maxima were at 395, 416, 439 nm for derivatives **9d** and **9i**, while **9h** had emission maxima

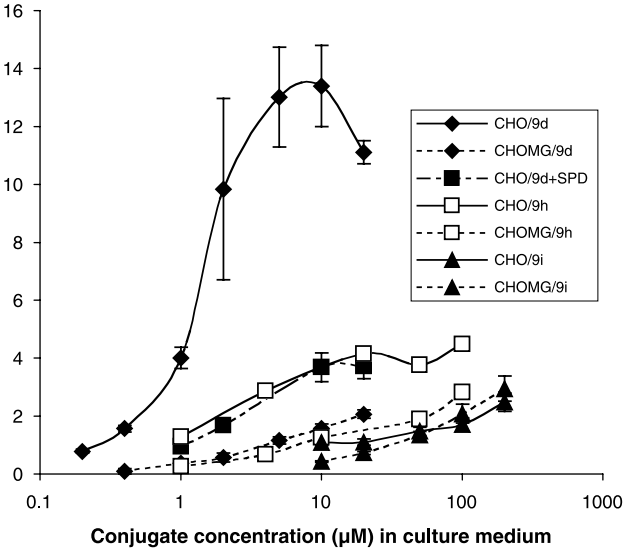

Fig. 2. Cell Uptake Studies with the N^1-(anthracen-9-ylalkyl)homospermidine series (Ant methyl **9d**, Ant ethyl **9h**, and Ant propyl **9i**) in CHO and CHO-MG cells. *For each graphed trend line*, the x-axis lists the concentration of the respective conjugate studied (**9d**, **9h**, or **9i**) in the particular cell line noted in the boxed legend, CHO or CHO-MG

at 391, 413, and 436 nm. Therefore, calibration curves allowed for quantification of conjugate import by quantifying the relative fluorescence emissions at these distinctive frequencies. The overall import results are listed in the y-axis and are expressed as nmoles conjugate/mg protein.

Results and discussion

In terms of the regiochemistry of the *N*-substituent, we first designed branched polyamines (e.g., **4**) due to the observation by Porter et al. that N^4-benzyl-spermidine was recognized by the PAT (Porter et al., 1985). In terms of the N-substituent design, we choose acridine and anthracene as polycyclic aromatic nuclei, which were both fluorescent and cytotoxic to cells (Phanstiel et al., 2000; Wang et al., 2001, 2002). In this manner, delivery of the arylpolyamine conjugate could be gauged via cytotoxicity measurements. Other studies confirmed the direct correlation between the degree of conjugate import and its IC_{50} value (e.g., the concentration of the drug required to kill 50% of the relative cell population) (Gardner et al., 2004).

The initial evaluation of branched systems **4a–e** demonstrated that the anthracenyl compounds (**4a** and **4b**) were more cytotoxic to murine leukemia (L1210) cells than the acridinyl conjugates (**4c** and **4d**) and that significant cell rescue was observed with **4e** upon the addition of spermidine **2** (100 μM) (Phanstiel et al., 2000; Wang et al., 2001). Moreover, bis-substituted adducts **5a–d**, containing large terminal *N*-alkylaryl groups, did not use the polyamine transporter (PAT) for cellular entry via 'spermidine-rescue' experiments (Wang et al., 2001). In this regard, mono-substituted polyamines were identified as preferred PAT ligands (Delcros et al., 2002; Wang et al., 2003a–c). Since the higher cytotoxicity of the anthryl probe provided greater sensitivity to our assay, we elected to use the 9-anthracenylmethyl group in the latter polyamine library **6–16**.

During construction of this library, Delcros and his collaborators demonstrated that linear acridine-polyamine conjugates were readily taken up by the polyamine transporter and demonstrated the utility of the Chinese hamster ovary (CHO) cell line in identifying PAT-selective materials (Delcros et al., 2002). Therefore, once synthesized, the new library was screened for cytotoxicity in CHO and CHO-MG cells.

Bioevaluation

Chinese hamster ovary (CHO) cells were chosen along with a mutant cell line (CHO-MG) in order to comment on how the synthetic conjugates gain access to cells (Delcros et al., 2002; Gardner et al., 2004). The CHO-MG cell line is polyamine-transport deficient and was isolated after selection for growth resistance to methylglyoxalbis (guanylhydrazone), MGBG, ($CH_3C[=N–NHC(=NH)NH_2]CH[=N–NHC(=NH)NH_2]$) using a single-step selection after mutagenesis with ethylmethanesulfonate (Mandel and Flintoff, 1978). The results are shown in Table 1.

For the purposes of this study, the parent CHO cell line represents a cell type with high PAT activity. In contrast, the CHO-MG mutant cell line represents cells with no PAT activity (Mandel and Flintoff, 1978) and provided a

Table 1. Biological evaluation of polyamine derivatives in CHO and CHO-MG cells[a]

Compd (tether)	CHO-MG IC_{50} in μM	CHO IC_{50} in μM	IC_{50} Ratio[b]
4b: Ant-methyl branched (5,4,3)[c]	51.3 (±19.9)	60.9 (±4.4)	0.8
6: Ant-methyl(*N*-butyl)	11.2 (±2.3)	10.5 (±2.0)	1.1
7: Ant-(butanediamine)	7.6 (±0.4)	7.7 (±0.5)	1
8: N^5-Ant-methyl(4,4)	86.6 (±7.1)	101.8 (±5.2)	0.9
9a: Ant-methyl(3,3)	3.4 (±0.5)	1.9 (±0.4)	1.8
9b: Ant-methyl(3,4)	8.8 (±1.2)	2.5 (±0.7)	3.5
9c: Ant-methyl(4,3)	9.5 (±1.1)	0.4 (±0.1)	24
9d: Ant-methyl(4,4)	66.7 (±4.1)	0.45 (±0.10)	148
9e: Ant-methyl(5,3)	10.1 (±1.2)	4.1 (±0.5)	2.5
9f: Ant-methyl(5,4)	57.3 (±2.9)	1.5 (±0.1)	38
9g: Ant-methyl(6,4)	38.2 (±2.4)	3.0 (±0.7)	12.7
9h: Ant-ethyl(4,4)	33.5 (±7.1)	9.8 (±1.1)	3.4
9i: Ant-propyl(4,4)	130.8 (±5.5)	130.1 (±7.1)	1
10a: Ant-methyl(3,3,4)	41.5 (±3.5)	44 (±0.0)	0.9
10b: Ant-methyl(3,4,3)	75.7 (±7.4)	59.7 (±6.5)	1.3
10c: Ant-methyl(3,4,4)	52.8 (±2.6)	31.1 (±7.3)	1.7
10d: Ant-methyl(3,5,4)	41.7 (±0.2)	34.9 (±1.3)	1.2
10e: Ant-methyl(4,4,3)	2.8 (±0.4)	4.0 (±1.4)	0.7
10f: Ant-methyl(4,4,4)	33.2 (±1.7)	10.6 (±0.0)	3.1
10g: Ant-methyl(5,4,3)	33.5 (±3.5)	18.1 (±3.5)	1.9
10h: Ant-methyl(5,4,4)	30.8 (±0.4)	9.9 (±1.6)	3.1
10i: Ant-methyl(5,5,4)	5.7 (±1.6)	4.0 (±0.8)	1.4
11: benzyl(4,4)	>1000	>1000	NA
12a: Nap-methyl(4,4)	>100	0.6 (±0.2)	>164
12b: Nap-ethyl(4,4)	106.1 (±11.2)	0.6 (±0.4)	177
12c: Nap-propyl(4,4)	>500[d]	>500[d]	NA
13: Pyr-methyl(4,4)	15.5 (±2.4)	0.46 (±0.05)	34
14: bis N^1,N^9-Ant-methyl(4,4)	1.2 (±0.1)	1.1 (±0.1)	1.1
15: Ant-methyl 4,cyclohexylene	17.4 (±2.8)	2.5 (±0.5)	7
16: Ant-methyl (4,3-hydroxyamino)	9.5 (±0.8)	9.1 (±0.4)	1

[a] Definitions used in Table 1, column 1: *Ant* anthracen-9-yl, *Nap* 1-naphthyl, *Pyr* pyren-1-yl; cells were incubated for 48 h with the respective conjugate

[b] The ratio denotes the (CHO-MG/CHO) IC_{50} ratio, a measure of PAT selectivity

[c] Derivative **4b** is a branched tetraamine, see Fig. 1

[d] 40% growth inhibition was observed for **12c** in both CHO and CHO-MG cell lines. No differential effect was observed

model for alternative modes of entry or action, which are independent of PAT. These alternative modes of entry include passive diffusion, utilization of another transporter, interactions on the outer surface of the plasma membrane or other membrane receptor interactions. Comparison of conjugate cytotoxicity in these two CHO lines provided an important screen for selective conjugate delivery via the PAT. For example, a conjugate with high utilization of the polyamine transporter would be very toxic to CHO cells, but less so to CHO-MG cells (Delcros et al., 2002; Wang et al., 2003a–c; Gardner et al., 2004). In short, highly selective PAT ligands should give high (CHO-MG/CHO) IC_{50} ratios.

As shown in Table 1, the controls (**6** and **7**) and compounds **8** (N^5-anthrylmethyl) and **14** (bis N^1,N^9-anthrylmethyl) had no preference for either CHO cell line and gave virtually identical IC_{50} values in both CHO-MG and CHO cells, respectively. This observation was consistent with these motifs entering the cell through non-PAT-mediated pathways. In this regard, neither substitution at the internal N^5-position (e.g., **6**) nor substitution at both terminal ends of the polyamine (e.g., **14**) provided a PAT-selective compound. However, terminally monosubstituted, linear polyamine motifs (e.g., **9d**) provided dramatic differences in cytotoxicity in these two cell lines (Wang et al., 2003a).

For example, the homospermidine derivative **9d** (IC_{50} values of **9d**: CHOMG: 66.7 μM, CHO: 0.45 μM; CHOMG/CHO IC_{50} ratio: 148), was a highly PAT-selective substrate (Wang et al., 2003a). Indeed, the CHOMG/CHO IC_{50} ratios in Table 1 suggested that PAT targeting is influenced by both the polyamine sequence and the location of the *N*-substituent. For example, terminal aminobutylation of 4,4-triamine **9d** to give 4,4,4-tetraamine **10e** significantly reduced its CHO cytotoxicity (IC_{50} CHO **10e**: 10.6 μM) and PAT selectivity (CHO-MG/CHO IC_{50} ratio for **10e**: 3.1). Further microscopy work, demonstrated that this was likely due to a 'sticky tetraamine' phenomenon, wherein tetraamines indiscriminantly bind to cell surface receptors, destabilize the membrane and possibly inhibit their own import (Wang et al., 2003b).

Certain triamines were identified as preferred PAT motifs due to the limited ability of their related tetraamines to release from the cell surface and the lower PAT selectivity observed with the tetraamine series (e.g., CHO-MG/CHO IC_{50} ratio **9d**: 148; **10e**: 3.1). Unlike the tetraamine **10e**, triamine **9d** was readily removed from the cell surface by a washing step with buffer (i.e., it binds reversibly) and revealed more triamine conjugate inside the cell per unit time (Wang et al., 2003b). Alteration of the triamine sequence in **9a**–**i**, demonstrated that the polyamine sequence was critical. Indeed, superior PAT-targeting was observed with the (4,4)-, (5,4)-, and (4,3)-triamine motifs: **9d** (CHO-MG/CHO IC_{50} ratio = 148), **9f** (38) and **9c** (24), respectively. Overall, the homospermidine (e.g., the 4,4-triamine sequence) was optimal and was kept constant throughout the remaining members of the library (Wang et al., 2003a–c; Gardner et al., 2004).

The influence of altering the N^1-substituent was exemplified in two series. First, the N^1 substituent was altered in terms of size via incremental increases in the aromatic component (i.e., benzyl **11**, naphthylmethyl **12a**, anthracenylmethyl **9d**, and pyrenylmethyl **13**), while still retaining the optimal homospermidine motif. As shown in Table 1, all members of this series were PAT-selective with CHO-MG/CHO IC_{50} ratios $\geq$34, except the benzyl derivative **11** (Wang et al., 2003a–c; Gardner et al., 2004).

Further experiments demonstrated that the benzyl derivative **11** was metabolized to free homospermidine, whereas the other members of this series were significantly more stable with only traces of homospermidine detected for the naphthyl case **12a** and none observed for **9d** (Wang et al., 2003b; Gardner et al., 2004). Therefore, in terms of pharmacophore design, the *N*-alkylaryl substituent needs to be of sufficient size to block the known N-dealkylation metabolic pathway (Bergeron et al., 1997).

In addition, the tether length connecting the aryl nucleus to the polyamine was systematically altered via the naphthyl series **12a**–**c** and the anthryl series **9d**, **9h**, and **9i**. As shown in Table 1, the naphthylmethyl (**12a**) and naphthylethyl (**12b**) conjugates were highly-selective PAT substrates with CHOMG/CHO IC_{50} ratios >164. However, the naphthylpropyl analogue (**12c**) had no PAT selectivity. A similar trend was evident in the anthryl series, wherein **9d** was highly PAT selective, whereas **9h** and **9i** were not. Thus, an additional methylene group was sufficient to dramatically alter the cytotoxicity profile of these N^1-substituted polyamines (Gardner et al., 2004). These findings are consistent with a molecular recognition event in PAT-mediated transport.

Subtle changes in the distances surrounding the N^1-position also resulted in dramatic changes in cytotoxicity in the CHO cell line. For example, maintaining the terminal anthracenylmethyl moiety, but altering the central alkylene tether length sequentially from butylene (**9d**), pentylene (**9f**) and hexylene (**9g**) resulted in decreasing CHOMG/CHO IC_{50} ratios (148, 38, and 12.7, respectively). As shown in Table 1, the conjugates became less PAT-selective and incrementally less toxic to CHO cells at longer ''central'' tether lengths (Gardner et al., 2004).

Prior work by others demonstrated that conformationally-restricted polyamines can significantly alter the cytotoxic response depending upon the structural element used to impart the rotational restriction (Valasinas et al., 2001). For example, introduction of *cis* and *trans* butene spacers in lieu of the more flexible, internal butylene chain generated tetraamines, which were less cytotoxic to cells than their aliphatic parent. However, introduction of a *cis* butene fragment near the terminal portion of the tetraamine gave enhanced cytotoxicity. Moreover, conformational restriction via introduction of small cycloalkyl motifs (e.g., cyclopropyl and cyclobutyl) were significantly more toxic than the aliphatic butylene parent and had lower systemic toxicities (Valasinas et al., 2001).

In this regard, 1,4-cyclohexylene adduct (**15**, Fig. 1) was synthesized and was shown to be significantly less PAT-selective than the free butylene adduct **9d** (Table 1) (Wang et al., 2003c). In addition, a recent report illustrated the hydroxylated polyamine motif as an alternative polyamine pharmacophore (Bergeron et al., 2000). However, model **16** revealed that at least for the hydroxylated spermidine motif, this alteration results in a dramatic loss of PAT selectivity compared to its parent 4,3-triamine adduct, **9c**, (Table 1). Therefore, in terms of pharmacophore design, the butylene tether provides an opportunity to tailor the cytotoxicity profile of the conjugate, while at the same time separating the ammonium ion charges at an optimal distance for PAT recognition (Bergeron et al., 1995, 1997; Gardner et al., 2004).

Transport

It was important to first demonstrate that the observed differences in cytotoxicity were due to changes in transport via PAT and not due to intrinsic differences in cytotoxicity. This feature was addressed via transport studies using fluorescent measurements of polyamine-conjugates (i.e., **9d**, **9h**, and **9i**) recovered from dosed CHO and CHO-MG cells (Gardner et al., 2004).

In order to relate the compelling IC_{50} trends to actual cell uptake of each conjugate, a series of fluorescence experiments to measure conjugate import were performed. In particular, the ''signature'' fluorescence profile associated with the anthracene nucleus was used to monitor conjugate uptake in CHO and CHO-MG cells (Fig. 2). Therefore, the anthracene component was easily tracked via its diagnostic fluorescence properties (see Materials and methods).

As shown in Fig. 2, there was a direct correlation between transport and the observed cytotoxicities of the **9d**, **9h**, and **9i** series. Indeed, derivative **9d**, which was shown to be the most PAT-selective of the series had the highest import rate (nmol/mg protein) and revealed dramatic uptake differences between CHO cells and the CHO-MG mutant (Fig. 2). Moreover, the import of **9d** was dramatically reduced in the presence of spermidine (SPD), (**2a**, a competitive antagonist for PAT) (Gardner et al., 2004).

Table 2. Cell selectivity profile for Ant-methyl-*N*-butyl control **6** and Ant-methyl **9d**[a]

Cell type/ conjugate	24 h IC_{50} (μM)	48 h IC_{50} (μM)	72 h IC_{50} (μM)
B16 (melanoma)/**6**	19.3 (±2.8)	21.31 (±2.18)	20.4 (±1.8)
Mel-A (normal melanocyte)/**6**	44.3 (±9.1)	32.80 (±4.64)	15.0 (±3.7)
B16 (melanoma)/**9d**	1.9 (±0.1)	1.1 (±0.1)	0.62 (±0.03)
Mel-A (normal melanocyte)/**9d**	16.5 (±2.0)	8.3 (±1.0)	6.5 (±1.2)

[a] IC_{50} values (μM) were determined at three time points (24, 48, and 72 h) in order to comment on the time-course toxicity of the polyamine-conjugate

The ability to selectively target melanoma cells was demonstrated using murine melanoma cells (B16) and normal melanocytes (Mel-A). As shown in Table 2, compound **9d** had 10-fold higher toxicity to the cancer cell line than the normal cell line after 72 h incubation.

Since the respective cell doubling times were different, IC_{50} ratios (**6**/**9d**) for each cell type were also compared. This interpretation revealed that the presence of the triamine vector in **9d** resulted in 10- to 33-fold higher cytotoxicity in B-16 cells, which have high PAT activity, than the control **6** (e.g., 72 h ratio: $20.4/0.62 = 33$). In contrast, the triamine vector in **9d** resulted in only 2- to 4-fold higher cytotoxicity in Mel-A cells than **6** (e.g., 72 h ratio: $15/6.5 = 2.3$). Therefore, the selectivity of this PAT-targeting strategy has been demonstrated in both normal and transformed cells in vitro (Gardner et al., 2004).

Future challenges

Future research will likely focus on three key areas: (a) understanding the initial polyamine recognition and import events (e.g., isolation of the mammalian polyamine transport proteins), (b) delineation of the intracellular trafficking of polyamine conjugates once they enter the cell (e.g., vesicular uptake and escape), and (c) optimization of interactions with the final cellular target (e.g., DNA binding events). Identification of the surface proteins and proteoglycans involved in polyamine recognition are an important first step (Belting et al., 1999, 2003). Indeed, the

Poulin group has presented a hypothetical model for polyamine uptake, which involves plasma membrane transport followed by capture by polyamine-sequestering vesicles (Soulet et al., 2002, 2004). More work is needed to understand how polyamines are stored and ''packaged'' for transit to various cellular organelles.

The collective work in this area to date has suggested that polyamines are transported across the cell membrane via a plasma membrane transporter, which may involve proteoglycans for polyamine recruitment. Once, inside the cell, the polyamines are then sequestered into vesicles. How polyamines escape from these vesicles and reach other cellular compartments remains a mystery and a worthy target for scientists interested in harnessing this PAT pathway for cell-selective drug delivery.

References

Aziz SM, Yatin M, Worthen DR, Lipke DW, Crooks PA (1998) A novel technique for visualising the intracellular localization and distribution of transported polyamines in cultured pulmonary artery smooth muscle cells. J Pharm Biomed Anal 17: 307–320

Azzam T, Eliyahu H, Shapira L, Linial M, Barenholz Y, Domb AJ (2002) Polysaccharide-oligoamine based conjugates for gene delivery. J Med Chem 45: 1817–1824

Belting M, Persson S, Fransson L-A (1999) Proteoglycan involvement in polyamine uptake. Biochem J 338: 317–323

Belting M, Mani K, Jönsson M, Cheng F, Sandgren S, Jonsson S, Ding K, Delcros J-G, Fransson L-A (2003) Glypican-1 is a vehicle for polyamine uptake in mammalian cells: a pivotal role for nitrosothiol-derived nitric oxide. J Biol Chem 278: 47181–47189

Bergeron RJ, McManis JS, Liu CZ, Feng Y, Weimar WR, Luchetta GR, Wu Q, Ortiz-Ocasio J, Vinson JRT, Kramer D, Porter C (1994) Antiproliferative properties of polyamine analogues: a structure-activity study. J Med Chem 37: 3464–3476

Bergeron RJ, McManis JS, Weimar WR, Schreier KM, Gao F, Wu Q, Ortiz-Ocasio J, Luchetta GR, Porter C, Vinson JRT (1995) The role of charge in polyamine analog recognition. J Med Chem 38: 2278–2285

Bergeron RJ, Feng Y, Weimar WR, McManis JS, Dimova H, Porter C, Raisler B, Phanstiel O (1997) A comparison of structure-activity relationships between spermidine and spermine analogue antineoplastics. J Med Chem 40: 1475–1494

Bergeron RJ, Müller R, Bussenius J, McManis JS, Merriman RL, Smith RE, Yao H, Weimar WR (2000) Synthesis and evaluation of hydroxylated polyamine analogues as antiproliferatives. J Med Chem 43: 224–235

Bergeron RJ, McManis JS, Franklin AM, Yao H, Weimar WR (2003) Polyamine-Iron Chelator Conjugate. J Med Chem 46: 5478–5483

Blagbrough IS, Geall AJ (1998) Homologation of polyamines in the synthesis of lipo-spermine conjugates and related lipoplexes. Tetrahedron Lett 39: 443–446

Byers TL, Wechter R, Nuttall ME, Pegg AE (1989) Expression of a human gene for polyamine transport in chinese hamster ovary cells. Biochem J 263: 745–752

Byers TL, Pegg AE (1990) Regulation of polyamine transport in chinese hamster ovary cells. J Cell Physiol 143: 460–467

Casero RA Jr, Woster PM (2001) Terminally alkylated polyamine analogues as chemotherapeutic agents. J Med Chem 44: 1–26

Cohen GM, Cullis P, Hartley JA, Mather A, Symons MCR, Wheelhouse RT (1992) Targeting of cytotoxic agents by polyamines: synthesis of a chloroambucil-spermidine conjugate. J Chem Soc Chem Commun 298–300

Covassin L, Desjardins M, Charest-Gaudreault R, Audette M, Bonneau MJ, Poulin R (1999) Synthesis of spermidine and norspermidine dimers as high affinity polyamine transport inhibitors. Bioorg Med Chem Lett 9: 1709–1714

Cullis PM, Merson-Davies L, Weaver R (1995) Conjugation of a polyamine to the bifunctional alkylating agent chlorambucil does not alter the preferred cross linking site in duplex DNA. J Am Chem Soc 117: 8033–8034

Cullis PM, Green RE, Merson-Davies L, Travis N (1999) Probing the mechanism of transport and compartmentalisation of polyamines in mammalian cells. Chem Biol 6: 717–729

Delcros J-G, Tomasi S, Carrington S, Martin B, Renault J, Blagbrough IS, Uriac P (2002) Effect of spermine conjugation on the cytotoxicity and cellular transport of acridine. J Med Chem 45: 5098–5111

Delcros J-G, Tomasi S, Duhieu S, Foucault M, Martin B, Le Roch M, Eifler-Lima V, Renault J, Uriac P (2006) Effect of polyamine homologation on the transport and biological properties of heterocyclic amidines. J Med Chem 49: 232–245

Gardner RA, Delcros J-G, Konate F, Breitbeil F III, Martin B, Sigman M, Huang M, Phanstiel O IV (2004) N^1-substituent effects in the selective delivery of polyamine-conjugates into cells containing active polyamine transporters. J Med Chem 47: 6055–6069

Gardner RA, Belting M, Svensson K, Phanstiel IV O (2007) Synthesis and transfection efficiencies of new lipophilic polyamines. J Med Chem 50: 308–318

Hasne M-P, Ullman B (2005) Identification and characterization of a polyamine permease from the protozoan parasite Leishmania major. J Biol Chem 280: 15188–15194

Heston WD, Uly L, Fair WR, Covey DF (1985) Cytotoxic activity of aziridinyl putrescine enhanced by polyamine depletion with alpha-difluoromethylornithine. Biochem Pharmacol 34: 2409–2410

Holley JL, Mather A, Wheelhouse RT, Cullis PM, Hartley JA, Bingham JP, Cohen GM (1992a) Targeting of tumor cells and DNA by a chlorambucil-spermidine conjugate. Cancer Res 52: 4190–4195

Holley JL, Mather A, Cullis PM, Symons MR, Wardman P, Watt RA, Cohen GM (1992b) Uptake and cytotoxicity of novel nitroimidazole-polyamine conjugates in Ehrlich ascites tumour cells. Biochem Pharmacol 43: 763–769

Huber M, Pelletier JG, Torossian K, Dionne P, Gamache I, Charestgandreault R, Audette M, Poulin R (1996) 2,2′-dithiobis(N-ethyl-spermine-5-carboxamide) is a high affinity, membrane-impermeant antagonist of the mammalian polyamine transport system. J Biol Chem 271: 27556–27563

Igarashi K, Kashiwagi K (1999) Polyamine transport in bacteria and yeast. Biochem J 344: 633–642

Kuksa V, Buchan R, Lin PKT (2000) Synthesis of polyamines, their derivatives, analogues and conjugates. Synthesis 9: 1189–1207

Lowry OH, Rosenbraugh NJ, Farr AL, Randall RJ (1951) Protein measurement with the Folin Phenol reagent. J Biol Chem 193: 265–275

Mandel JL, Flintoff WF (1978) Isolation of mutant mammalian cells altered in polyamine transport. J Cell Physiol 97: 335–344

Martin B, Possémé F, Le Barbier C, Carreaux F, Carboni B, Seiler N, Moulinoux J-P, Delcros J-G (2001) N-Benzylpolyamines as vectors of boron and fluorine for cancer therapy and imaging: synthesis and biological evaluation. J Med Chem 44: 3653–3664

Martin B, Possémé F, Le Barbier C, Carreaux F, Carboni B, Seiler N, Moulinoux J-P, Delcros J-G (2002) (Z)-1,4-diamino-2-butene as a vector of boron, fluorine, or iodine for cancer therapy and imaging: synthesis and biological evaluation. Bioorg Med Chem 10: 2863–2871

Marton LJ, Levin VA, Hervatin SJ, Koch-Weser J, McCann PP, Sjoerdsma A (1981) Potentiation of the antitumor therapeutic effects of 1,3-bis(2-chloroethyl)-1-nitrosurea by alpha-difluoromethylornithine, an ornithine decarboxylase inhibitor. Cancer Res 41: 4426–4431

Mitchell JLA, Simkus CL, Thane TK, Tokarz P, Bonar MM, Frydman B, Valasinas AL, Reddy VK, Marton LJ (2004) Antizyme induction mediates feedback limitation of the incorporation of specific polyamine analogues in tissue culture. Biochem J 384: 271–279

Phanstiel O IV, Price HL, Wang L, Juusola J, Kline M, Shah SM (2000) The effect of polyamine homologation on the transport and cytotoxicity properties of polyamine-(DNA-intercalator) conjugates. J Org Chem 65: 5590–5599

Porter C, Miller J, Bergeron RJ (1984) Aliphatic chain-length specificity of the polyamine transport system in ascites L1210 leukemia cells. Cancer Res 44: 126–128

Porter CW, Cavanaugh PF, Ganis B, Kelly E, Bergeron RJ (1985) Biological properties of N^4- and N^1,N^8-spermidine derivatives in cultured L1210 leukemia cells. Cancer Res 45: 2050–2057

Seiler N, Dezeure F (1990) Polyamine transport in mammalian cells. Int J Biochem 22: 211–218

Seiler N, Delcros J-G, Moulinoux JP (1996) Polyamine transport in mammalian cells. An update. Int J Biochem Cell Biol 128: 843–861

Soulet D, Covassin L, Kaouass M, Charest-Gaudreault R, Audette M, Poulin R (2002) Role of endocytosis in the internalisation of spermidine-C2-BODIPY, a highly fluorescent probe of polyamine transport. Biochem J 367: 347–357

Soulet D, Gagnon B, Rivest S, Audette M, Poulin R (2004) A fluorescent probe of polyamine transport accumulates into intracellular acidic vesicles via a two-step mechanism. J Biol Chem 279: 49355–49366

Stark PA, Thrall BD, Meadows GG, Abdul-Monem MM (1992) Synthesis and evaluation of novel spermidine derivatives as targeted cancer chemotherapeutic agents. J Med Chem 35: 4264–4269

Valasinas A, Sarkar A, Reddy VK, Marton LJ, Basu HS, Frydman B (2001) Conformationally restricted analogues of 1N,14N-bisethylhomospermine (BE-4-4-4): synthesis and growth inhibitory effects on human prostate cancer cells. J Med Chem 44: 390–403

Wang L, Price HL, Juusola J, Kline M, Phanstiel O IV (2001) The Influence of polyamine architecture on the transport and topoisomerase II inhibitory properties of polyamine DNA-intercalator conjugates. J Med Chem 44: 3682–3691

Wang C, Abboud KA, Phanstiel O IV (2002) Synthesis and characterization of N^1-(4-toluenesulfonyl)-N^1-(9-anthracenemethyl)triamines. J Org Chem 67: 7865–7868

Wang C, Delcros J-G, Biggerstaff J, Phanstiel O IV (2003a) Synthesis and biological evaluation of N^1-(anthracen-9-ylmethyl)triamines as molecular recognition elements for the polyamine transporter. J Med Chem 46: 2663–2671

Wang C, Delcros J-G, Biggerstaff J, Phanstiel O IV (2003b) Molecular requirements for targeting the polyamine transport system: synthesis and biological evaluation of polyamine-anthracene conjugates. J Med Chem 46: 2672–2682

Wang C, Delcros J-G, Cannon L, Konate F, Carias H, Biggerstaff J, Gardner RA, Phanstiel O IV (2003c) Defining the molecular requirements for the selective delivery of polyamine-conjugates into cells containing active polyamine transporters. J Med Chem 46: 5129–5138

Yuan ZM, Egorin MJ, Rosen DM, Simon MA, Callery PS (1994) Cellular pharmacology of N1- and N8-aziridinyl analogues of spermidine. Cancer Res 54: 742–748

Authors' address: Otto Phanstiel IV, Department of Chemistry, University of Central Florida, P.O. Box 162366, Orlando, FL 32816-2366, USA, Fax: +1-407-823-2252, E-mail: ophansti@mail.ucf.edu